

ORIGINAL ARTICLE

Prenatal Exposure to Autism-Specific Maternal Autoantibodies Alters Proliferation of Cortical Neural Precursor Cells, Enlarges Brain, and Increases Neuronal Size in Adult Animals

Verónica Martínez-Cerdeño^{1,2,5}, Jasmin Camacho^{1,5}, Elizabeth Fox^{2,4}, Elaine Miller^{1,5}, Jeanelle Ariza^{1,5}, Devon Kienzle^{1,5}, Kaela Plank^{1,5}, Stephen C. Noctor^{2,3}, and Judy Van de Water^{2,4}

¹Department of Pathology and Laboratory Medicine, ²MIND Institute, ³Department of Psychiatry and Behavioral Sciences, UC Davis, Sacramento, CA 95817, USA, ⁴Department of Rheumatology/Allergy and Clinical Immunology, UC Davis, Davis, CA 95616, USA, and ⁵Institute for Pediatric Regenerative Medicine and Shriners Hospitals for Children Northern California, Sacramento, CA, 95817, USA

Address correspondence to Verónica Martínez-Cerdeño, 2425 Stockton Blvd, Sacramento, CA 95817, USA. Email: vmartinezcerdeno@ucdavis.edu

Abstract

Autism spectrum disorders (ASDs) affect up to 1 in 68 children. Autism-specific autoantibodies directed against fetal brain proteins have been found exclusively in a subpopulation of mothers whose children were diagnosed with ASD or maternal autoantibody-related autism. We tested the impact of autoantibodies on brain development in mice by transferring human antigen-specific IgG directly into the cerebral ventricles of embryonic mice during cortical neurogenesis. We show that autoantibodies recognize radial glial cells during development. We also show that prenatal exposure to autism-specific maternal autoantibodies increased cellular proliferation in the subventricular zone (SVZ) of the embryonic neocortex, increased adult brain size also and weight, and increased the size of adult cortical neurons. We propose that prenatal exposure to autism-specific maternal autoantibodies directly affects radial glial cell development and presents a viable pathologic mechanism for the maternal autoantibody-related prenatal ASD risk factor.

Key words: autism, brain size, maternal autoantibody, neurogenesis, radial glial cells

Introduction

Autism spectrum disorder (ASD) encompasses a group of neurodevelopmental disorders defined by a pattern of qualitative abnormalities in reciprocal social interaction, communication, and repetitive interests and behaviors ([American Psychiatric Association 1994](#)). Current estimates indicate that the prevalence of ASD in the USA is 1 in 68 for children 8 years of age ([Frieden 2012](#)) with behaviors ranging from severe impairments with

no verbal communication and severe mental disability to highly functioning individuals who may suffer from mild alterations in social approach and communication. While the etiology of idiopathic ASD is unknown, there are likely numerous distinct etiologies associated with an autism diagnosis given the wide range of behavioral manifestations.

A strong association between maternal antibody reactivity toward fetal brain and an outcome of autism in the child has been independently identified by several groups ([Dalton et al. 2003](#);

Singer et al. 2008), and a particular pattern of reactivity that is unique to mothers of children with ASD has been identified (Braunschweig et al. 2008; Braunschweig, Duncanson et al. 2012). The same pattern of reactivity has been observed in prospectively collected mid-gestation blood samples from mothers who subsequently gave birth to a child with autism (Croen et al. 2008), supporting the possibility that these antibodies may have a direct effect on neurodevelopment in utero.

In humans and other mammals, maternal IgG isotype antibodies readily cross the placenta to equip the immunologically naïve fetus with a subset of antibodies that provide the fetus with passive protection against a myriad of possible infectious agents (Garty et al. 1994). These maternal IgG antibodies persist for up to 6 months after birth (Heininger et al. 2006). However, along with immunoprotective IgG antibodies, autoantibodies that react to fetal “self”-proteins also cross the placenta. Gestational transfer of maternal antibodies with reactivity to fetal proteins is an established cause of congenital abnormalities in the context of maternal autoimmune disorders (Tincani et al. 2006). Therefore, brain-reactive antibodies have the potential to exert substantial effects on the prenatal developing brain through their interaction with the target antigens. This interaction can take several forms including receptor activation, receptor blockade, or reducing the effective level of a soluble protein.

We have previously demonstrated that the maternal autoantibodies are reactive to the identical proteins in both human and mouse fetal brain and produce developmental delays and behavioral alterations in mice exposed to the maternal autoantibodies during development (Braunschweig, Golub et al. 2012; Camacho et al. 2014). These findings suggest the evolutionary conservation of these self-antigens and indicate that the mouse is an appropriate model for the proposed research. However, the mechanism by which these antibodies exert their effect in the developing brain *in vivo* remains unknown. We hypothesized that *in utero* exposure to autism-specific maternal autoantibodies would change the normal patterns of cortical development and alter cortical cell properties.

Materials and Methods

IgG Preparation

Banked plasma from mothers of children with autism who have IgG reactivity to the 37-kDa (lactate dehydrogenase or LDH) and 73-kDa (stress-induced phosphoprotein 1 or STIP1; collapsin response mediator protein 1 or CRMP1) fetal brain proteins (MAU^{ab}, *n* = 4) and plasma from mothers of typically developing children who do not have fetal brain-reactive IgG (MTD^{ab} *n* = 5) was used for all experiments. The samples were obtained from the CHARGE Study at the University of California, Davis M.I.N.D. Institute. Children enrolled in the CHARGE study underwent thorough behavioral evaluations by expert clinicians to confirm diagnosis. Following characterization of the maternal autoantibody profile by fetal brain western blot, IgG was purified from plasma under sterile conditions using Protein A/G columns and dialyzed against sterile saline. Prepared IgG samples were tested for bacterial contamination using an LPS-detecting turbidity assay, and only samples verified to be sterile and pyogen free were used. For immunohistochemistry, purified IgG was biotinylated under sterile conditions according to manufacturer's instructions (Thermo Scientific #21425, EZ-Link™ Sulfo-NHS-Biotinylation Kit). The amount of a 10 mM Sulfo-NHS-Biotin solution needed for the respective IgG protein solutions was

calculated and was subsequently added, so that each IgG protein solution contained a 20 molar excess of biotin. The reaction was incubated on ice for 2 h. Following incubation, each solution was dialyzed against sterile saline using Slide-A-Lyzer® MINI Dialysis Devices (Thermo Scientific #88401) to remove excess non-reacted and hydrolyzed biotin reagent. In line with the procedure, each sample was added to the device and placed in a conical tube containing the buffer, and incubated on an orbital shaker for 2 h at 4°C. The buffer was then replaced, and the samples were dialyzed at 4°C overnight against sterile phosphate-buffered saline.

Animals

The UC Davis Institutional Animal Care and Use Committee approved all experiments with mice. Pregnant adult female Swiss Webster mice were purchased from Charles River. We used female Swiss Webster because, based in our previous experience (Noctor et al. 2001; Noctor et al. 2004; Noctor et al. 2008), embryos from this strain are easier to inject *in utero* and the survival rate is higher than that in other mice strains. All animals were housed at the University of California, Davis animal facilities. The number of animals used in each experiment was minimized. Pregnant dams were randomly assigned to receive injections of MAU^{ab} or MTD^{ab}.

Intraventricular Injection

Timed pregnant mice were anesthetized on embryonic day 14 or 16, an abdominal incision made through the skin and the abdominal muscular layer, and temporarily exposed the uterine horns. 0.5–1.0 µL containing 10 µg of purified MAU^{ab} or MTD^{ab} was then injected directly into the cerebral ventricle of each embryo by passing a 33-gauge micropipette through the uterine wall and into the cerebral ventricle. All pups were injected in each pregnant mouse. The uterine horns were replaced, and the muscular layer and skin sutured closed.

Immunohistochemistry

The fetal brains were removed after 2 h or 2 days, post-fixed for 24 h in 4% paraformaldehyde at 4°C, and coronal 50-µm-thick slices were made on a vibratome. The sections were blocked in 10% donkey serum (GIBCO), 0.1% Triton X-100 (Sigma), and 0.2% gelatin (Sigma), rinsed, and incubated for 24 h at room temperature in the primary antibodies (mouse anti-phosphorylated vimentin (4A4) 1 : 500 (MBL), mouse anti-Pax6 1 : 50 (Abcam), rabbit anti-Pax6 (Covance, 1 : 1000), and rabbit anti-Tbr2 1 : 500 (Abcam). After rinsing, the sections were incubated in the appropriate secondary antibody in 2% fetal donkey serum, 0.02% Triton X-100, (w/v) 0.04% gelatin, and DAPI 1 : 1000 (Roche). Secondary antibodies were conjugated to Dylight 488, Cy3/Dylight 549, or Cy5/Dylight 649 (Jackson Laboratories). Slices were then rinsed and cover-slipped with Mowiol.

Stereology

We quantified the number of specific cell types in the murine cerebral cortex using the optical fractionator design, and the volume of neuronal soma using the nucleator design, using an Olympus microscope with StereoInvestigator Optical Fractionator Workflow (MicroBrightField). The neocortex boundaries were defined at low magnification with a ×2 objective. Cell numbers were quantified within layers II through VI of the neocortex with a ×100 oil objective. We analyzed a minimum of 200 cells in

10 sections per quantification experiment. To prevent sampling bias, we measured post-processing tissue thickness at each sampling. We quantified a cell if the nucleolus came into focus within the dissector counting frame and did not count if the nucleolus was inside the guard zone, touching the exclusion line, or outside the counting frame. We carried out the optimal sampling scheme using the population estimator followed by a sampling of each case. We used the population estimate to determine grid size, counting frame, and number of sections to sample to reach a coefficient of error of less than 10% (Gundersen et al. 1988; Gundersen et al. 1999).

Imaging

Slices were imaged on a Nikon A1 Confocal Microscope. Single optical planes were used for analysis of co-expression. Analysis and quantification were performed on the Nikon software and in Photoshop CS3 (Adobe).

Statistics

Data are reported as mean \pm s.e.m. We performed t-Tests with a two-tailed *P*-value test to statistically compare the number of cells positive for specific markers between groups using GraphPad Prism (GraphPad Software, Inc.).

Results

MAU^{ab} Penetrates into the Cortical Parenchyma and Binds to Radial Glial Cells in the VZ

To demonstrate that IgG penetrated the cortical parenchyma after administration and the cell types recognized directly by maternal autoantibodies specific of autism (MAU^{ab}), we biotinylated MAU^{ab} or maternal autoantibodies of mothers with typically developing children (MTD^{ab}) and injected it into the cerebral ventricles of E14 pregnant mice. MAR^{ab} included all IgGs present in the maternal plasma including the MAR^{ab} specific to autism. MTD^{ab} included all IgGs present in the maternal plasma that did not contain autoantibodies specific to autism. We perfused litters 2 days or 2 h after the injection and removed the brains. We then amplified the biotin signal in the developing cortical plate and obtained staining in the ventricular zone (VZ) in tissue perfused 2 h after injection (Fig. 1A), but not on that perfused 2 days after injection. Strong staining was noted in cells with morphology characteristic of neuronal stem cells known as radial glial (RG) cells (Fig. 1A,C–G). We performed immunohistochemical co-localization with neuronal (MAP2) and glial (Pax6, GFAP, Olig2, and vimentin) cell markers. The cells that stained by biotin amplification only co-localized with vimentin, further suggesting the RG cell nature of these autoantibody targeted cells (Fig. 1H). Of note, we did not observe positive signal when purified biotinylated MTD^{ab} IgG was used (Fig. 1B).

MAU^{ab} Increases Cell Proliferation in the Subventricular Zone of the Developing Cerebral Cortex

To determine the direct effects of MAU^{ab} on the developing brain, we performed single injections of MAU^{ab} isolated from 4 individual mothers or MTD^{ab} isolated from 5 individual mothers, into the cerebral ventricles of E14 mouse embryos in utero. This gestation date represents the middle stages of cortical neurogenesis in mouse (Takahashi et al. 1996). The total MAU^{ab} from each mother were not pooled but used individually. Our approach delivers IgGs directly to the location of cortical precursor cells that

line the margins of the embryonic cerebral ventricles. All the embryos in the dam, except for the most distal embryo in the right and left uterine horns, were injected. Most of the embryos survived, and we randomly selected 3 or 4 embryos per litter to be analyzed. Fifteen embryos from 4 pregnant dams injected with MAU^{ab}, and 20 embryos from 5 pregnant dams injected with MTD^{ab} were analyzed. Two days following the IgG antibody injection, enough time for progenitor cells that were in contact with the ventricular surface at the time of the injection to divide and for daughter cells to migrate out the VZ (Noctor et al. 2004), embryos were perfused, and the number and distribution of neural precursor cells in the cerebral cortex of prenatal mice exposed to MAU^{ab} or MTD^{ab} was determined.

The fetal brains were removed, sectioned into coronal slices, and immunostained with antibodies to label actively dividing precursor cells (phosphorylated vimentin, 4A4, Fig. 2A,D), RG cells and translocating RG cells (Pax6, Fig. 2A,B), and intermediate progenitor (IP) cells (Tbr2, Fig. 2A,C). We chose 4A4 as a mitotic maker because it only labels dividing neurogenic progenitor cells, and not all the dividing cell population such as endothelial cells, as is the case for other mitotic markers such as pH3 and Ki67. In addition, 4A4 labels dividing cells in all the M-phase stages and not other mitotic phases, in contrast to Ki67 that labels also cells in G2 and S-phase, or PH3 that does not label all the M-phase cells and labels some G2 cells (Weissman et al. 2003). The number of immunopositive precursor cells was quantified in 300- μ m-wide rectangular bins that spanned from the ventricular surface to the pia with the most lateral side of the bin located at the telencephalo-diencephalic junction and the most ventral border parallel to the ventricular surface. Cells were quantified in one of every six 50- μ m coronal sections spanning the whole rostro-caudal extent of the cerebral cortex. We averaged the number of each cell type per bin in all the analyzed slices of each embryo. Then, we averaged the number obtained for of each cell type in each embryo from the same mother and used this final number for statistical analysis.

We found that the number of 4A4+ mitotic precursor cells in the cerebral cortex of E16 mice prenatally exposed to MAU^{ab} on E14 was significantly increased by 30% when compared with the MTD^{ab} group ($P = 0.03$, Fig. 3G). We analyzed the number of 4A4+ precursor cells that were located in the VZ or the SVZ of animals in each group and found that increased proliferation in the SVZ accounted for the difference. The number of 4A4+ precursor cells in the SVZ was increased 43% in the MAU^{ab}-treated embryos compared with MTD^{ab}-treated embryos ($P = 0.02$, Fig. 3G), but was not significantly different in the VZ of MAU^{ab}-treated embryos.

The population of mitotic precursor cells in the SVZ includes both Tbr2+ IP cells and Pax6+ RG cells that have translocated to the SVZ where they continue dividing (Fietz et al. 2010; Hansen et al. 2010; Martínez-Cerdeño et al. 2012). We co-immunostained coronal sections with antibodies against 4A4, and against the transcription factors Pax6 or Tbr2, and quantified the number of 4A4+ cells expressing Tbr2 or Pax6 (Fig. 2E,F). We found no difference in the number of Tbr2+ cells, or in the number of Tbr2/4A4 double-positive mitotic cells between the MAU^{ab} and MTD^{ab} groups (Fig. 2H). We next quantified and compared the number of Pax6+ cells and Pax6/4A4 double-positive cells between the 2 treatment groups. There was no significant change in the total number of Pax6+ cells between groups, nor in the total number of Pax6/4A4 double-positive cells between groups (Fig. 3I). However, we found a 62% increase in the number of Pax6/4A4 cells in the SVZ of mice in the MAU^{ab} group ($P = 0.01$, Fig. 2J). Pax6+ cells present in the SVZ represent translocating RG cells. Thus, we inferred that the increased number of 4A4+

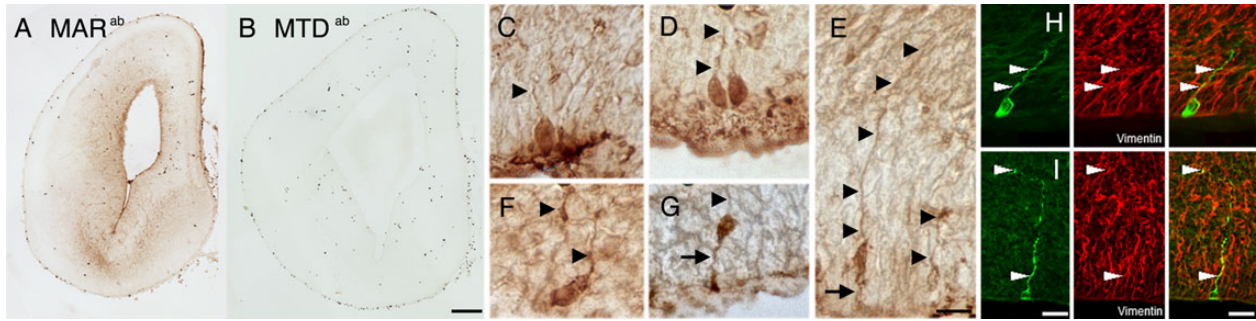


Figure 1. Biotinylated-MAR^{ab} or MTD^{ab} were injected into the cerebral ventricles of E14 embryonic mice. (A,B) Coronal sections run in parallel for biotin amplification showed biotin-MAR^{ab}-labeled cells in the VZ and SVZ (A), whereas biotin-MTD^{ab} did not label cells (B). Note: erythrocytes produced nonspecific labeling in MAR^{ab} and MTD^{ab}. (C-G) RG neural stem cells were positive for biotin-MAR^{ab}. Arrowheads indicate RG pial fibers; arrows indicate RG ventricular process. (H,I) biotin-MAR^{ab}+ cells (green) co-localized with the RG cell marker vimentin (red). Scale bars: (A,B) 100 μ m; (C-H) 10 μ m.

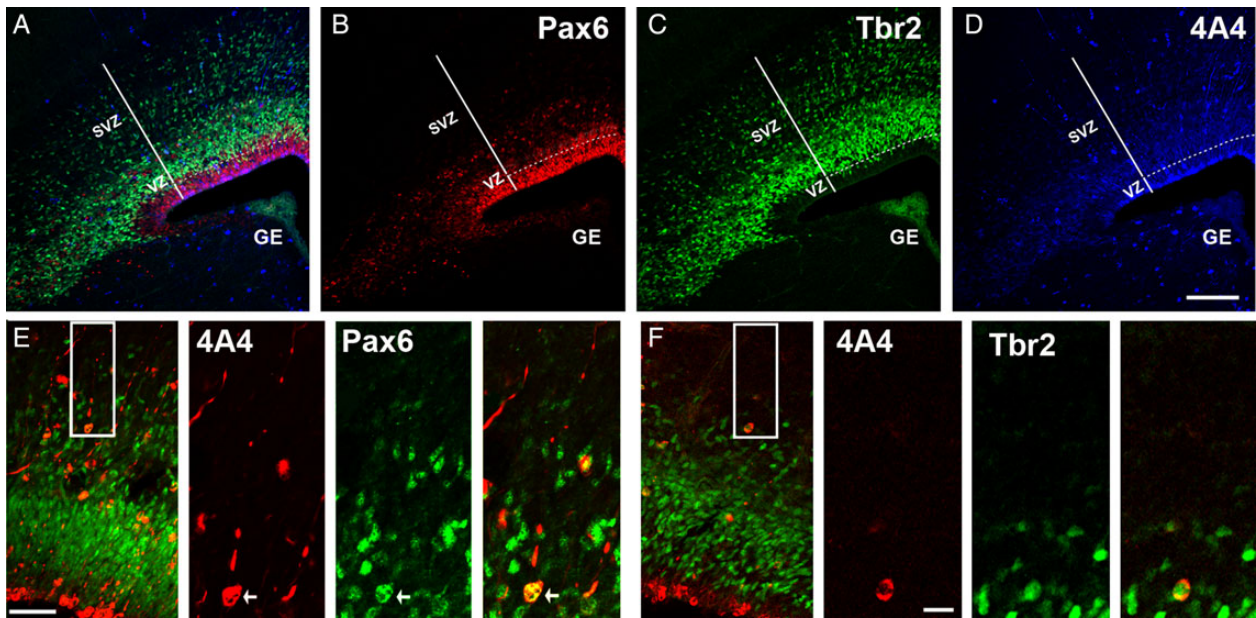


Figure 2. Analysis of precursor cell number. Maternal MAU^{ab} and MTD^{ab} IgGs were injected in utero in E14 mice, and precursor cell number in the cerebral cortex was quantified 2 days later at E16. (A) Triple immunostaining for Pax6 (red, B), Tbr2 (green, C), and 4A4 (blue, D). (E) Proliferative precursor cell types located in the SVZ of the E16 developing cortex. Inset indicates region of higher power images to the right. Mitotic translocating RG cells were identified by expression of the mitotic cell marker 4A4 (red), presence of a pial directed fiber, and expression of Pax6 (green). (F) Proliferative precursor cell types in the E16 developing cortex. Inset indicates region of higher power images to the right. Mitotic intermediate progenitor cells were identified by expression of the mitotic cell marker 4A4 (red), and expression of Tbr2 located in the SVZ (green). Calibration bar: (A-D) 250 μ m; (E,F) 100 μ m and 25 μ m, respectively.

dividing cells in the MAU^{ab} group represented dividing Pax6+ RG cells that had precociously translocated from the VZ into the SVZ. We repeated the experiments during later stages of neurogenesis and injected MAU^{ab} and control MTD^{ab} into pregnant mice at E16 and analyzed the results at E18. We obtained results similar to the previous experiments since the number of 4A4+ cells and the number of 4A4+/Pax6+ cells in the SVZ were significantly increased by 36% and 96%, respectively. As in the earlier time point, none of the other variables analyzed varied between groups.

We qualitatively assessed the titer of the IgG samples from each human mother by correlating western blot staining intensity (see Supplementary Fig. 1) with effects on cortical development. We found that samples with higher IgG titer (e.g., ASD4) had a more pronounced effect on cell proliferation. In contrast, samples with lower IgG titer (e.g., ASD3) had a comparatively reduced effect on proliferation. These results support the concept that higher IgG titer of MAU^{ab} can be more deleterious to brain development.

We further stained the tissue with caspase 6 to label cell death and did not find any significant difference in the number of caspase 6+ cells when compare embryos injected with MAU^{ab} or MTD^{ab}, indicating that any change found in the number of cells was due to proliferation and not to cell death.

MAU^{ab} Increase Cell Proliferation in Extra-Cortical Areas

We next tested whether MAU^{ab} increased precursor cell proliferation in other regions of the brain. We quantified the number of 4A4+ precursor cells in the ganglionic eminence in 300- μ m-wide rectangular bins that spanned through the proliferative zones. We found that the number of dividing precursor cells in the SVZ of the ganglionic eminence was significantly increased by 65% in the MAU^{ab} group versus the MTD^{ab} group ($P = 0.03$). We did not detect a difference in the total number of 4A4+ precursor cells ($P = 0.3$), which again suggests that MAU^{ab} induces a precocious shift of RG precursor cells from the VZ into the SVZ (Fig. 4).

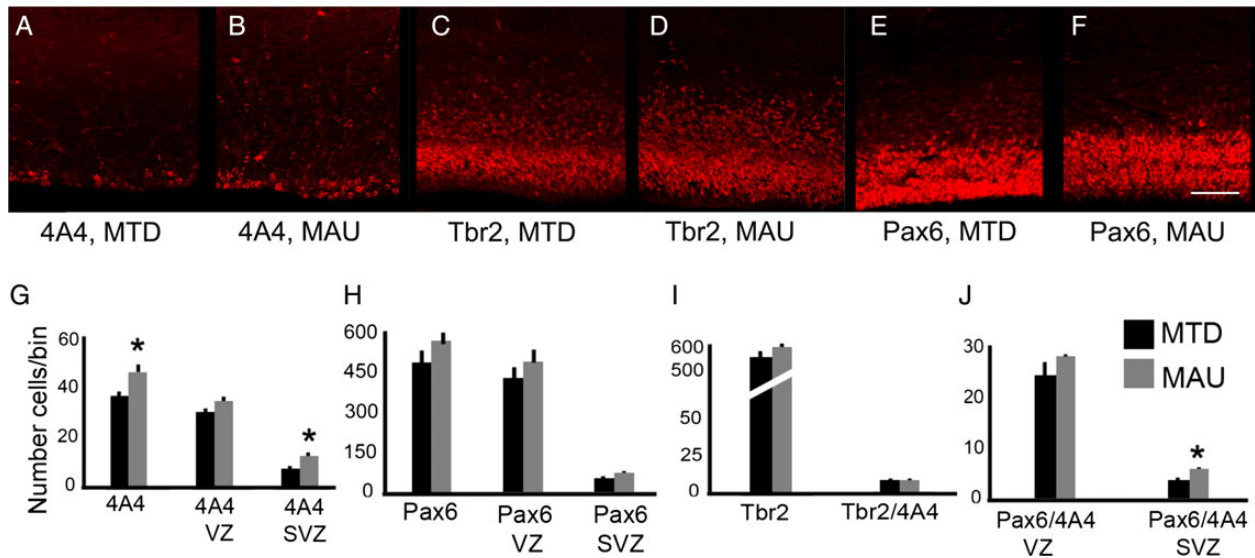


Figure 3. Prenatal exposure to MAU^{ab} increases the number of proliferative Pax6⁺ precursor cells in the SVZ. Maternal MAU^{ab} and MTD^{ab} IgGs were injected in utero in E14 mice, and precursor cell number in the cerebral cortex was quantified 2 days later at E16. (A,B,G) MAU^{ab} treatment increased the number of 4A4⁺ mitotic precursor cells in the SVZ ($P = 0.02$), but not in the VZ of the developing neocortex. (C-F, H,I) The total number of Tbr2⁺ and Pax6⁺ precursor cells did not differ in mice exposed to MAU^{ab} compared with mice exposed to MTD^{ab}. (J) The number of mitotic Tbr2⁺ precursor cells (Tbr2⁺/4A4⁺) was not different in mice exposed to MAU^{ab} versus MTD^{ab}. However, the number of mitotic Pax6⁺ precursor cells (Pax6⁺/4A4⁺) was significantly increased in the SVZ ($P = 0.01$), but not in the VZ of the developing neocortex of mice exposed to MAU^{ab} versus MTD^{ab}. Calibration bar: 50 μ m.

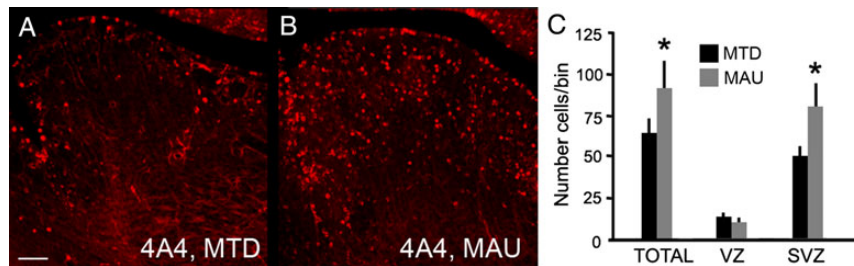


Figure 4. MAU^{ab} treatment significantly increased the number of mitotic precursor cells in the SVZ of the ganglionic eminence. (A,B) E16 murine ganglionic eminence (GE) 2 days after injection with either MAU^{ab} and MTD^{ab} IgGs at E14. (C) The number of 4A4⁺ mitotic precursor cells was significantly increased in the SVZ ($P = 0.03$), but not in the VZ of the developing GE after exposure to MAU^{ab} compared with MTD^{ab} exposure. Calibration bar: 100 μ m.

MAU^{ab} Do not Alter Microglial Cell Number or Level of Activation

Microglia, the innate immune cell of the central nervous system, colonize the prenatal cerebral cortex during the neurogenic stages of development (Rezaie and Male 1999; Cunningham et al. 2013). We have recently discovered that microglia regulate the number of cortical precursor cells in the normally developing neocortex and that inflammatory activation of the maternal immune system impacts the function of fetal microglia, subsequently altering the number of neural precursor cells in the prenatal neocortex (Cunningham et al. 2013). We therefore tested whether the presence of passively transferred MAU^{ab} could impact the native immune cells in the prenatal cerebral cortex by quantifying the number and/or activation state of microglial cells in the prenatal neocortex. MAU^{ab} and MTD^{ab} from 4 plasma samples were each injected individually into the cerebral ventricles of 14 embryos. Embryos were perfused 2 days post-injection, fetal brains removed, sectioned coronally, and immunostained with Iba1 antibodies to label microglia (Cunningham et al. 2013). The number of Iba1⁺ microglia was quantified in

300- μ m-wide rectangular bins that spanned from the ventricle to the pia. The state of activation of microglial cells was determined by quantifying cell morphology on a four-point scale (Rezaie and Male 1999). Two days after administration, we found no significant differences in the number or state of activation of microglial cells between treatment groups (cell number: $P = 0.91$; activation: $P = 0.60$; not shown). These data suggest that changes in the activation state or total numbers of fetal microglial cells were not apparent 2 days after injection of the maternal autoantibodies, and thus, did not likely contribute to the altered number of precursor cells we observed in the MAU^{ab} group.

MAU^{ab} Increases the Size and Weight of Adult Brains, as Well as the Size of Neurons in the Adult Cerebral Cortex

We next tested whether prenatal exposure to maternal autoantibodies impacted the histology, cellular composition, and neuroanatomy of the mature cerebral cortex. MAU^{ab} and MTD^{ab} were injected into the cerebral ventricles of E14 embryos in 4 pregnant dams (2 MAU^{ab} and 2 MTD^{ab}). Embryos were born naturally

yielding 9 MAU^{ab} and 9 MTD^{ab} male offspring. At 6 months of age, we sacrificed the animals and dissected out the whole brains for measurement.

For weight and length studies, we perfused animals with saline for 10 min to eliminate the blood content and dissected the brains by doing a straight incision between the cerebral cortex and the olfactory bulbs, removing the bulbs, and between the cerebral cortex and the cerebellum, removing the cerebellum and all other cerebral tissue caudal to the incision. After blocking, we dried the excess phosphate-buffered saline and weighed brains on a high precision balance. Brains of adult male animals prenatally exposed to MAU^{ab} weighed more than those exposed to MTD^{ab} (MAU^{ab}: 365.26 ± 5.06 mg; MTD^{ab}: 352.73 ± 2.41 mg; $P = 0.002$, Fig. 5A). We measured the rostro-caudal, and medio-lateral width of all brains. To determine the lengths, we imaged the brains next to a scale and processed images with Image J. We measured rostro-caudal length as the distance between the most anterior and the most posterior borders of the cerebral cortex, and the medio-lateral length as the greater medio-lateral distance in the right hemisphere. There was a significant increase in the rostro-caudal length of brains from animals exposed to MAU^{ab} compared with those exposed to MTD^{ab} (MAU^{ab}: 8.40 ± 0.16 mm; MTD^{ab}: 7.75 ± 0.25 mm; $P = 0.05$). We noted an increase in the medio-lateral width in the brains of MAU^{ab}-exposed male animals compared with MTD^{ab}-exposed male animals, but this increase was not quite significant (Fig. 5B,C).

We next quantified the total number of neuronal and glial cells in the cerebral cortex of animals in each group. Coronal sections were cut and immunostained with antibodies against NeuN for neurons, S100 for astrocytes, and Olig2 for oligodendrocytes, then counterstained with DAPI (Fig. 6A). We quantified the total number of cortical cells, and the total number of each cell type in the neocortex using stereology (dissector probe). We quantified the number of cells within the layer II to VI of the neocortex, excluding the arcuate cortex and the paleocortex, using stereology. We did not find significant differences in the number of each cell type between the MAU^{ab} or MTD^{ab} groups (DAPI: $P = 0.47$; NeuN: $P = 0.52$; S100: $P = 0.91$; Olig2: $P = 0.84$; Fig. 6A,B).

However, we also quantified the cellular volume of NeuN+ cells within the neocortex using stereology (nucleator probe) and found that the somal volume of NeuN+ cortical cells was

greater in the MAU^{ab}-exposed group compared with the MTD^{ab} group (MAU^{ab}: 1295.7 ± 95.1 μm³; MTD^{ab}: 926.2 ± 83.4 μm³; $P = 0.01$; Fig. 6C). This increase in volume did not seem to be specific to a single cortical layer but widespread throughout layer II to VI of the cerebral cortex.

In summary, we found that the brains of mice prenatally exposed to MAU^{ab} were bigger, weighed more, and that cortical neuron volume was greater in the MAU^{ab} group. However, the number of cortical cells, regardless of cell type, did not differ between groups.

Discussion

Our previous studies identified paired maternal IgG antibody reactivity to 2 fetal brain protein bands at ~37 and 73 kDa in 11.5% (7/61) of mothers of children with autism (MAU^{ab}), which was absent (0/62) in mothers of typically developing children (MTD^{ab}) (Braunschweig et al. 2011). In a replication study, we confirmed these findings in an expanded cohort, while demonstrating that paired maternal reactivity to the 37- and 73-kDa antigens was associated with increased severity of language deficits in the offspring (Braunschweig et al. 2011). Furthermore, we found antibody reactivity to an additional pair of protein bands in the region of 39 and 73 kDa that associated significantly with increased irritability and self-injurious behavior in the children of positive mothers. We have also found that the functional MET promoter variant rs1858830 “C” allele was highly associated with the presence of MAU^{ab} (Heuer et al. 2011). Limited passive transfer animal models of gestational exposure to human IgG antibodies suggest that MAU^{ab} may directly influence behaviors in the offspring reminiscent of those observed in children with autism (Braunschweig, Golub et al. 2012; Martin et al. 2008; Camacho et al. 2014). Further, we have now identified the target antigens recognized by these autoantibodies, which are associated with MAR autism (Braunschweig et al. 2013). For the current study, we focused on maternal plasma samples that contained antibodies to the primary targets in MAR autism: LDH, STIP1, and CRMP1. Thus, while we now know the identity of the autoantibody targets, the mechanism by which these antibodies exert their effect in the developing brain *in vivo* remains unknown. In the current study, we applied purified human IgGs directly into the cerebral ventricles of embryonic mice. We showed, for the first time, the effects of direct prenatal exposure to human maternal fetal brain-specific autoantibodies on precursor cells, and adult cortical histology and anatomy in a murine model.

During cortical development, the proliferative cells that produce cortical neurons and glial cells are located in proliferative zones that surround the ventricular lumen: the VZ, which is adjacent to the ventricle, and the SVZ, which is superficial to the VZ (Bystron et al. 2008; Boulder Committee 1970). RG cells are primary cortical precursor cells that are located in the VZ, express the transcription factor Pax6 (Gotz et al. 1998; Englund et al. 2005), and generate neurons, IP cells, and astrocytes (Noctor et al. 2001; Noctor et al. 2004; Noctor et al. 2008). During neurogenic stages of cortical development, RG cells produce IP cells that populate the SVZ, express the transcription factor Tbr2 (Englund et al. 2005), and generate cortical neurons (Noctor et al. 2004; Noctor et al. 2008). RG cells have also been shown to detach from the ventricle and translocate through the overlying SVZ toward the cortical plate (Schmechel and Rakic 1979; Voigt 1989; Noctor et al. 2004). RG cell translocation has been documented in live time-lapse recordings of GFP-expressing cells (Noctor et al. 2004; Noctor et al. 2008), and more recently through time-lapse imaging followed by Pax6 immunostaining to definitively show

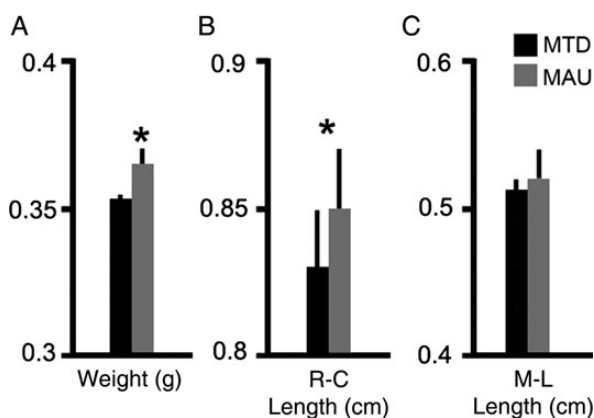


Figure 5. Prenatal MAU^{ab} exposure increased brain size and weight. (A) Brains of adult animals prenatally exposed to MAU^{ab} weighed more than those exposed to MTD^{ab} (MAU^{ab}: 365.26 ± 5.06 mg; MTD^{ab}: 352.73 ± 2.41 mg; $P = 0.002$). (B, C) Rostro-caudal length (R-C) was increased in brains from animals exposed to MAU^{ab} compared with those exposed to MTD^{ab}. Medio-lateral length (M-L) was increased but the difference was not a significant.

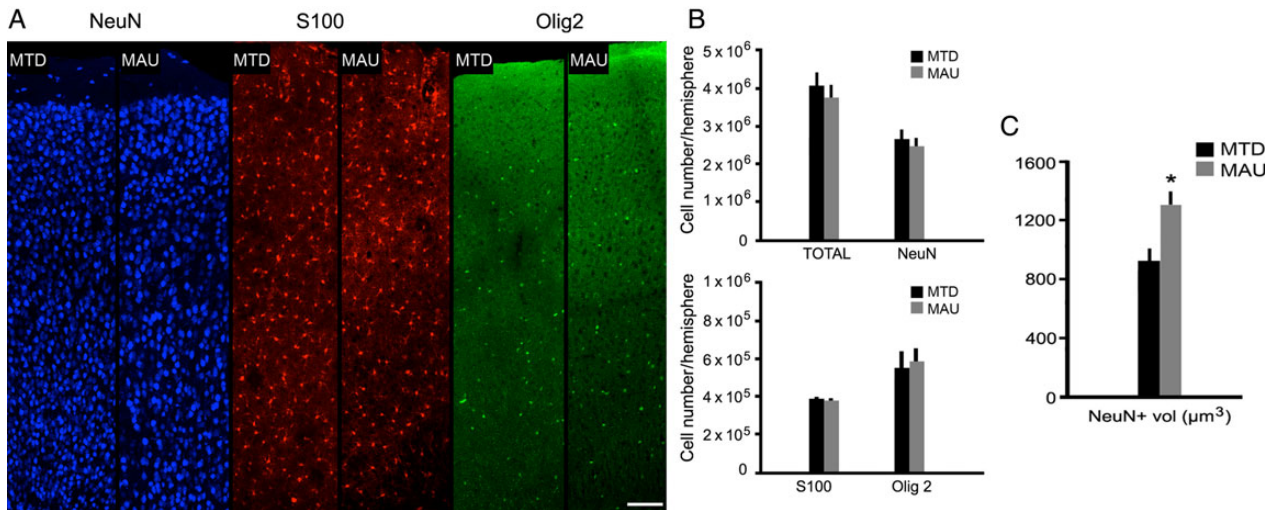


Figure 6. Stereological analysis of cortical cell number and somal size in the adult cerebral cortex of animals that were prenatally exposed to MAU^{ab} or MTD^{ab} at E14. (A,B) The number of Neu⁺ cells (neurons), S100⁺ cells (astrocytes), and Olig2⁺ cells (oligodendrocytes) did not differ between MAU^{ab} and MTD^{ab} mice. (C) However, the size of the NeuN⁺ cells was increased in the MAU^{ab}-exposed animals compared with those exposed to MTD^{ab} ($P = 0.01$). Calibration bar: (A–D). 100 µm.

the translocation of Pax6⁺ precursor cells out of the VZ (Hansen et al. 2010; Martínez-Cerdeño et al. 2012). However, the developmental stage when RG cells translocate away from the VZ varies by species. For example, in rat, Pax6⁺ RG cells begin translocating from the VZ during late stages of neurogenesis, and at the onset of gliogenesis (Fig. 7A). In contrast, RG cells translocate during early stages of neurogenesis in the fetal macaque (Martínez-Cerdeño et al. 2012), and fetal human cortex (Fietz et al. 2010; Hansen et al. 2010), (Fig. 7B). We found that in prenatal mice exposed to MAU^{ab}, RG cells precociously detached from the ventricle and translocated away from the VZ much earlier than in controls. Furthermore, the MAU^{ab}-induced RG translocation occurred at nearly the same stage of development as in the macaque (Fig. 7C). Translocation of RG cells into the overlying SVZ has been proposed as a mechanism to boost neuron production (Smart et al. 2002; Hansen et al. 2010). In our experiments, a single dose exposure to MAU^{ab} did not produce adult mice with an increased number of cells in the cerebral cortex. This could result from a shorter neurogenic period in MAU^{ab}-treated mice, or from increased cell death occurring in the first postnatal weeks.

The premature translocation of RG cells into the SVZ of MAU^{ab}-exposed animals could impact the trajectory and/or timing of neuronal migration into the developing cortical plate. Premature arrival of newly generated cells into the cortical gray matter could alter the connectional properties of developing circuits, as well as, cellular morphology, which could partially explain the increased cortical neuron size in MAU^{ab}-exposed animals. Alteration in stem cell proliferation and the migration of newborn cells have previously been linked to autism. Casanova has proposed that the increased number of minicolumns he previously described in autistic subjects could result from increased germinal cell divisions (Casanova et al. 2003; Casanova et al. 2013; Casanova 2014).

We noted a significant increase in the size of neuronal soma and a significant increase in weight of the brain of animals prenatally exposed to MAU^{ab}. These findings are in line with a recent report showing that maternal autoantibodies are associated with brain enlargement in a subgroup of children with ASD (Nordahl et al. 2013) and suggest that our animal model may replicate important facets of human neuropathology in ASDs. Interestingly, a

related non-human primate passive transfer model whereby purified human IgG from mothers with specific reactivity to the 37/73-kDa fetal brain proteins was passively transferred into pregnant Rhesus monkeys demonstrated that the male offspring of the ASD-IgG but not the control IgG exposed animals had enlarged brains similar to children with ASD (Bauman et al. 2013). These data, combined with the findings herein, provide further evidence that maternal autoantibodies to fetal brain proteins might be related to the reported changes in brain growth trajectory in ASD. Recent work by others has shown that temporal lobe epilepsy is characterized by normal cell numbers but with increased cell size and altered connectional properties that correlate with dysfunction (Bothwell et al. 2001). In addition, altered expression of genes that regulate cell size, such as mTOR, have been implicated in ASD (García-Penas and Carreras-Saez 2013) and are reflected in changes in cell morphology and cognitive functioning (Alayev and Holz 2013). Further studies are needed to clarify the relationship between changes in neuronal cell morphology and the behavioral aspects of ASD.

We did not observe changes in the number or apparent activation state of fetal microglia in the cerebral cortex 2 days after a single exposure to the MAU^{ab}. While this finding might suggest that the interplay between the immune system and the developing brain is not altered in this animal model, our paradigm allowed us to investigate only the immediate and longer-term impact of a single exposure to maternal MAU^{ab} and does not fully replicate changes in maternal immune functioning that accompany production of MAU^{ab} in the human condition in which the developing fetus is likely exposed to the maternal autoantibodies over a longer period of gestation. This could potentially be associated with altered levels of maternal, placental, and/or fetal cytokines that have been associated with (Deverman and Patterson 2009; Meyer 2013) and that impact neural precursor cell function (Monje and Palmer 2003; Cunningham et al. 2013).

Our data are consistent with the concept that autoantibodies present in women during gestation recognize proteins in the developing fetal brain, and exposure to these autoantibodies may be correlated with the etiology of ASD in a specific subset of children (Braunschweig et al. 2013). The increased proliferation of Pax6⁺ precursor cells in the SVZ of the developing cerebral cortex

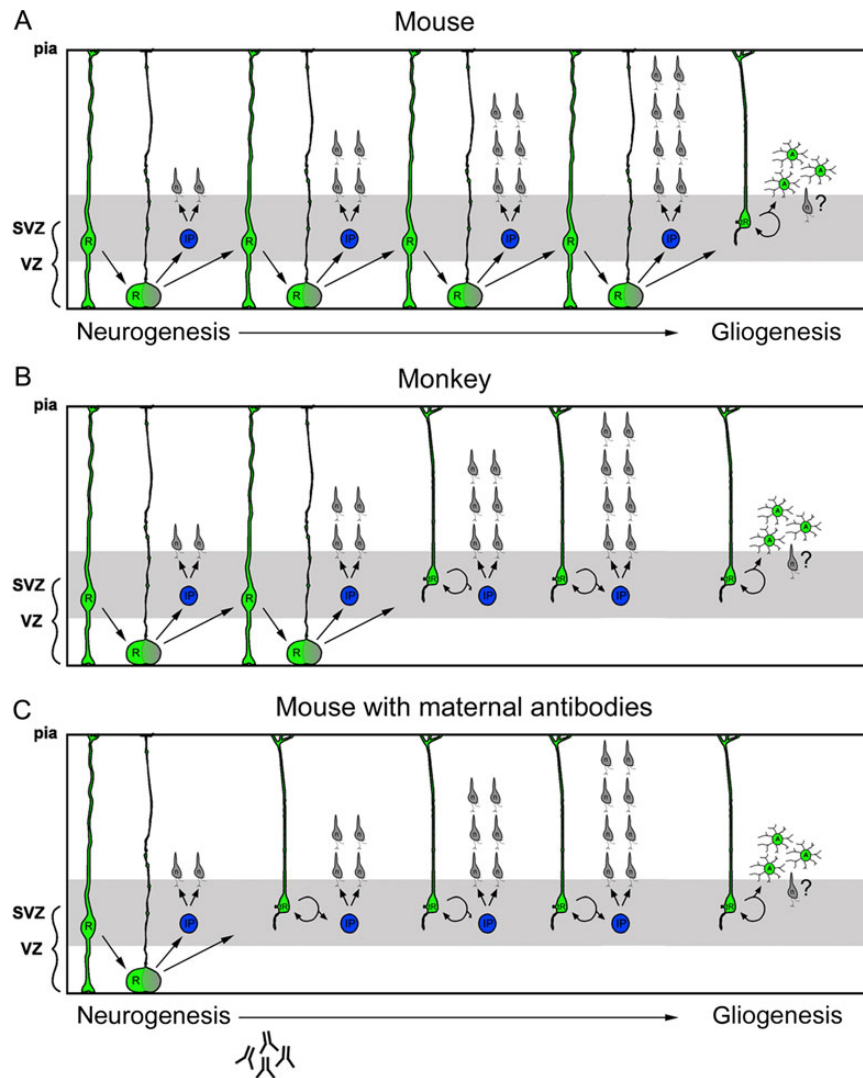


Figure 7. Scheme depicting how prenatal MAU^{ab} impacts precursor cell function during development of the cerebral cortex. RG cells detach from the ventricle and translocate their soma from the VZ into the overlying SVZ. However, the stage of development at which RG cells translocate into the SVZ is tightly regulated and varies by species. (A) In mouse, Pax6+ RG cells begin translocating from the VZ during later stages of neurogenesis. (B) In macaque, RG cells begin translocating into the SVZ soon after the start of neurogenesis. (C) In the prenatal mouse neocortex that has been exposed to MAU^{ab}, RG cells precociously detach from the ventricle and translocate away from the VZ into the SVZ much earlier than normal. Prenatal treatment with MAU^{ab} produces RG translocation in the mouse at nearly the same stage of cortical development as occurs in the macaque, changing the normal pattern and timing of the neurogenic process.

during middle stages of neurogenesis in several regions of the developing CNS, including the ganglionic eminence in the basal forebrain, suggests that maternal autoantibodies specific for proteins critical for neuronal development are pathologically significant. In the MAU^{ab} group, we found altered patterns of proliferation in the dorsal neocortex where excitatory projection neurons are generated, and also in the ganglionic eminence where most of interneurons are produced. These data imply that maternal autoantibodies will affect both neuronal populations and could potentially impact the balance of excitation to inhibition, which has been proposed to play a role in the cognitive dysfunction in ASD (Rubenstein and Merzenich 2003).

As noted, we discovered that the specific fetal brain proteins recognized by the maternal autoantibodies we used in our experiments are LDH, STIP1, and CRMP1. ASD children from mothers with specific reactivity to these proteins had elevated stereotypical behaviors compared with ASD children from mothers lacking these antibodies (Braunschweig et al. 2013). STIP1, first detected

in the developing nervous system starting at E8 (Hajj et al. 2009), has been shown to mediate neuritogenesis in cultured hippocampal neurons (Lopes et al. 2005; Roffe et al. 2010). STIP1 also modulates astrocyte proliferation (Arantes et al. 2009) and proliferation of glioblastoma cells (Erlich et al. 2007). The group of CRMPs 1-5 are thought to contribute to semaphorin-induced growth cone collapse (Quach et al. 2004). More specifically, CRMP1 is highly expressed in the developing brain and is required for proper cell migration, growth cone collapse, and cell survival (Charrier et al. 2003; Quach et al. 2004; Charrier et al. 2006; Kurnellas et al. 2010). The enzyme LDH is found in the rodent fetal brain (Hashimoto et al. 2008) where it functions in cellular metabolism. Although autoantibodies targeting LDH have not yet been shown to directly play a role in altering neurodevelopment, these autoantibodies have been identified in sera from individuals exposed to the industrial solvent trichloroethylene (Liu et al. 2009).

To further study the impact of maternal autoantibodies on neural stem cell proliferation in autism, we will focus our future

studies on individual autoantibodies affinity purified against LDH, STIP1 (previously associated with proliferative regulation), and CRMP1 (associated with cell migration), to provide a clearer picture of the pathogenic mechanisms involved in maternal antibody related autism.

Supplementary Material

Supplementary material can be found at: <http://www.cercor.oxfordjournals.org/>.

Funding

V.M.C. received support from the NIMH (MH094681) and Shriners Hospitals, S.C.N. from the NIMH (MH101188), and V.D.W. from P01 ES011269.

Notes

Conflict of Interest: None declared.

References

- Alayev A, Holz MK. 2013. mTOR signaling for biological control and cancer. *J Cell Physiol.* 228(8):1658–1664.
- American Psychiatric Association D. 1994. Diagnostic and Statistical Manual of Mental Disorders. 4th ed. Washington, DC.
- Arantes C, Nomizo R, Lopes MH, Hajj GN, Lima FR, Martins VR. 2009. Prion protein and its ligand stress inducible protein 1 regulate astrocyte development. *Glia.* 57(13):1439–1449.
- Bauman MD, Iosif AM, Ashwood P, Braunschweig D, Lee A, Schumann CM, Van de Water J, Amaral DG. 2013. Maternal antibodies from mothers of children with autism alter brain growth and social behavior development in the rhesus monkey. *Transl Psychiatry.* 3:e278.
- Bothwell S, Meredith GE, Phillips J, Staunton H, Doherty C, Grigorenko E, Glazier S, Deadwyler SA, O'Donovan CA, Farrell M. 2001. Neuronal hypertrophy in the neocortex of patients with temporal lobe epilepsy. *J Neurosci.* 21(13):4789–4800.
- Boulder Committee. 1970. Embryonic vertebrate central nervous system: revised terminology. *Anatom Record.* 166(2):257–261.
- Braunschweig D, Ashwood P, Krakowiak P, Hertz-Picciotto I, Hansen R, Croen LA, Pessah IN, Van de Water J. 2008. Autism: maternally derived antibodies specific for fetal brain proteins. *Neurotoxicology.* 29(2):226–231.
- Braunschweig D, Duncanson P, Boyce R, Hansen R, Ashwood P, Pessah IN, Hertz-Picciotto I, Van de Water J. 2012. Behavioral correlates of maternal antibody status among children with autism. *J Autism Dev Disord.* 42(7):1435–1445.
- Braunschweig D, Golub MS, Koenig CM, Qi L, Pessah IN, Van de Water J, Berman RF. 2012. Maternal autism-associated IgG antibodies delay development and produce anxiety in a mouse gestational transfer model. *J Neuroimmunol.* 252(1–2):56–65.
- Braunschweig D, Krakowiak P, Duncanson P, Boyce R, Hansen RL, Ashwood P, Hertz-Picciotto I, Pessah IN, Van de Water J. 2013. Autism-specific maternal autoantibodies recognize critical proteins in developing brain. *Transl Psychiatry.* 3:e277.
- Bystron I, Blakemore C, Rakic P. 2008. Development of the human cerebral cortex: boulder committee revisited. *Nat Rev Neurosci.* 9(2):110–122.
- Camacho J, Jones K, Miller E, Ariza J, Noctor S, Van de Water J, Martinez-Cerdeno V. 2014. Embryonic intraventricular exposure to autism-specific maternal autoantibodies produces alterations in autistic-like stereotypical behaviors in offspring mice. *Behav Brain Res.* 266C:46–51.
- Casanova MF. 2014. Autism as a sequence: from heterochronic germinal cell divisions to abnormalities of cell migration and cortical dysplasias. *Med Hypotheses.* 83(1):32–38.
- Casanova MF, Buxhoeveden D, Gomez J. 2003. Disruption in the inhibitory architecture of the cell minicolumn: implications for autism. *Neuroscientist.* 9(6):496–507.
- Casanova MF, El-Baz AS, Kamat SS, Dombroski BA, Khalifa F, Elnakib A, Soliman A, Allison-McNutt A, Switala AE. 2013. Focal cortical dysplasias in autism spectrum disorders. *Acta Neuropathol Commun.* 1(1):67.
- Charrier E, Mosinger B, Meissirel C, Aguera M, Rogemond V, Reibel S, Salin P, Chounlamountri N, Perrot V, Belin MF, et al. 2006. Transient alterations in granule cell proliferation, apoptosis and migration in postnatal developing cerebellum of CRMP1^{-/-} mice. *Genes Cells.* 11(12):1337–1352.
- Charrier E, Reibel S, Rogemond V, Aguera M, Thomasset N, Honnorat J. 2003. Collapsin response mediator proteins (CRMPs): involvement in nervous system development and adult neurodegenerative disorders. *Mol Neurobiol.* 28(1):51–64.
- Croen LA, Braunschweig D, Haapanen L, Yoshida CK, Fireman B, Grether JK, Kharrazi M, Hansen RL, Ashwood P, Van de Water J. 2008. Maternal mid-pregnancy autoantibodies to fetal brain protein: the early markers for autism study. *Biol Psychiatry.* 64(7):583–588.
- Cunningham CL, Martinez-Cerdeno V, Noctor SC. 2013. Microglia regulate the number of neural precursor cells in the developing cerebral cortex. *J Neurosci.* 8(5):e63848.
- Dalton P, Deacon R, Blamire A, Pike M, McKinlay I, Stein J, Styles P, Vincent A. 2003. Maternal neuronal antibodies associated with autism and a language disorder. *Ann Neurol.* 53(4):533–537.
- Deverman BE, Patterson PH. 2009. Cytokines and CNS development. *Neuron.* 64(1):61–78.
- Englund C, Fink A, Lau C, Pham D, Daza RA, Bulfone A, Kowalczyk T, Hevner RF. 2005. Pax6, Tbr2, and Tbr1 are expressed sequentially by radial glia, intermediate progenitor cells, and postmitotic neurons in developing neocortex. *J Neurosci.* 25(1):247–251.
- Erlich RB, Kahn SA, Lima FR, Muras AG, Martins RA, Linden R, Chiarini LB, Martins VR, Moura Neto V. 2007. STI1 promotes glioma proliferation through MAPK and PI3K pathways. *Glia.* 55(16):1690–1698.
- Fietz SA, Kelava I, Vogt J, Wilsch-Brauninger M, Stenzel D, Fish JL, Corbeil D, Riehn A, Distler W, Nitsch R, et al. 2010. OSVZ progenitors of human and ferret neocortex are epithelial-like and expand by integrin signaling. *Nat Neurosci.* 13(6):690–699.
- Frieden TR. 2012. Prevalence of Autism Spectrum Disorders – Autism and Developmental Disabilities Monitoring. US Department of Health and Human Services Centers for Disease Control and Prevention. 61(3):1–18.
- Garcia-Penas JJ, Carreras-Saez I. 2013. Autism, epilepsy and tuberous sclerosis complex: a functional model linked to mTOR pathway. *Rev Neurol.* 56(Suppl 1):S153–S161.
- Garty BZ, Ludomirsky A, Danon YL, Peter JB, Douglas SD. 1994. Placental transfer of immunoglobulin G subclasses. *Clin Diagn Lab Immunol.* 1(6):667–669.
- Gotz M, Stoykova A, Gruss P. 1998. Pax6 controls radial glia differentiation in the cerebral cortex. *Neuron.* 21(5):1031–1044.

- Gundersen HJ, Bendtsen TF, Korbo L, Marcussen N, Moller A, Nielsen K, Nyengaard JR, Pakkenberg B, Sorensen FB, Vesterby A, et al. 1988. Some new, simple and efficient stereological methods and their use in pathological research and diagnosis. *APMIS*. 96(5):379–394.
- Gundersen HJ, Jensen EB, Kieu K, Nielsen J. 1999. The efficiency of systematic sampling in stereology – reconsidered. *J Microsc*. 193(Pt 3):199–211.
- Hajj GN, Santos TG, Cook ZS, Martins VR. 2009. Developmental expression of prion protein and its ligands stress-inducible protein 1 and vitronectin. *J Comp Neurol*. 517(3):371–384.
- Hansen DV, Lui JH, Parker PR, Kriegstein AR. 2010. Neurogenic radial glia in the outer subventricular zone of human neocortex. *Nature*. 464(7288):554–561.
- Hashimoto T, Hussien R, Cho HS, Kaufer D, Brooks GA. 2008. Evidence for the mitochondrial lactate oxidation complex in rat neurons: demonstration of an essential component of brain lactate shuttles. *PLoS One*. 3(8):e2915.
- Heininger U, Desgrandchamps D, Schaad UB. 2006. Seroprevalence of Varicella-Zoster virus IgG antibodies in Swiss children during the first 16 months of age. *Vaccine*. 24(16):3258–3260.
- Heuer L, Braunschweig D, Ashwood P, Van de Water J, Campbell DB. 2011. Association of a MET genetic variant with autism-associated maternal autoantibodies to fetal brain proteins and cytokine expression. *Transl Psychiatry*. 1:e48.
- Kurnellas MP, Li H, Jain MR, Giraud SN, Nicot AB, Ratnayake A, Heary RF, Elkabes S. 2010. Reduced expression of plasma membrane calcium ATPase 2 and collapsin response mediator protein 1 promotes death of spinal cord neurons. *Cell Death Differ*. 17(9):1501–1510.
- Liu J, Xing X, Huang H, Jiang Y, He H, Xu X, Yuan J, Zhou L, Yang L, Zhuang Z. 2009. Identification of antigenic proteins associated with trichloroethylene-induced autoimmune disease by serological proteome analysis. *Toxicol Appl Pharmacol*. 240(3):393–400.
- Lopes MH, Hajj GN, Muras AG, Mancini GL, Castro RM, Ribeiro KC, Brentani RR, Linden R, Martins VR. 2005. Interaction of cellular prion and stress-inducible protein 1 promotes neurogenesis and neuroprotection by distinct signaling pathways. *J Neurosci*. 25(49):11330–11339.
- Martin LA, Ashwood P, Braunschweig D, Cabanlit M, Van de Water J, Amaral DG. 2008. Stereotypies and hyperactivity in rhesus monkeys exposed to IgG from mothers of children with autism. *Brain Behav Immun*. 22(6):806–816.
- Martinez-Cerdeno V, Cunningham CL, Camacho J, Antczak JL, Prakash AN, Cziep ME, Walker AI, Noctor SC. 2012. Comparative analysis of the subventricular zone in rat, ferret and marmoset: evidence for an outer subventricular zone in rodents. *PLoS One*. 7(1):e30178.
- Meyer U. 2013. Developmental neuroinflammation and schizophrenia. *Prog Neuropsychopharmacol Biol Psychiatry*. 42:20–34.
- Monje ML, Palmer T. 2003. Radiation injury and neurogenesis. *Curr Opin Neurol*. 16(2):129–134.
- Noctor SC, Flint AC, Weissman TA, Dammerman RS, Kriegstein AR. 2001. Neurons derived from radial glial cells establish radial units in neocortex. *Nature*. 409(6821):714–720.
- Noctor SC, Martinez-Cerdeno V, Ivic L, Kriegstein AR. 2004. Cortical neurons arise in symmetric and asymmetric division zones and migrate through specific phases. *Nat Neurosci*. 7(2):136–144.
- Noctor SC, Martinez-Cerdeno V, Kriegstein AR. 2008. Distinct behaviors of neural stem and progenitor cells underlie cortical neurogenesis. *J Comp Neurol*. 508(1):28–44.
- Nordahl C, Braunschweig D, Iosif A, Lee A, Rogers S, Ashwood P, Amaral D, Van de Water J. 2013. Maternal autoantibodies are associated with abnormal brain enlargement in a subgroup of children with autism spectrum disorder. *Brain Behav Immun*. 30:61–65.
- Quach TT, Duchemin AM, Rogemond V, Aguera M, Honnorat J, Belin MF, Kolattukudy PE. 2004. Involvement of collapsin response mediator proteins in the neurite extension induced by neurotrophins in dorsal root ganglion neurons. *Mol Cell Neurosci*. 25(3):433–443.
- Rezaie P, Male D. 1999. Colonisation of the developing human brain and spinal cord by microglia: a review. *Microsc Res Tech*. 45(6):359–382.
- Roffe M, Beraldo FH, Bester R, Nunziante M, Bach C, Mancini G, Gilch S, Vorberg I, Castilho BA, Martins VR, et al. 2010. Prion protein interaction with stress-inducible protein 1 enhances neuronal protein synthesis via mTOR. *Proc Natl Acad Sci USA*. 107(29):13147–13152.
- Rubenstein JL, Merzenich MM. 2003. Model of autism: increased ratio of excitation/inhibition in key neural systems. *Genes Brain Behav*. 2(5):255–267.
- Schmechel DE, Rakic P. 1979. A Golgi study of radial glial cells in developing monkey telencephalon: morphogenesis and transformation into astrocytes. *Anat Embryol (Berl)*. 156(2):115–152.
- Singer HS, Morris CM, Gause CD, Gillin PK, Crawford S, Zimmerman AW. 2008. Antibodies against fetal brain in sera of mothers with autistic children. *J Neuroimmunol*. 194(1-2):165–172.
- Smart IH, Dehay C, Giroud P, Berland M, Kennedy H. 2002. Unique morphological features of the proliferative zones and postmitotic compartments of the neural epithelium giving rise to striate and extrastriate cortex in the monkey. *Cereb Cortex*. 12(1):37–53.
- Takahashi T, Nowakowski RS, Caviness VS Jr. 1996. Interkinetic and migratory behavior of a cohort of neocortical neurons arising in the early embryonic murine cerebral wall. *J Neurosci*. 16(18):5762–5776.
- Tincani A, Nuzzo M, Motta M, Zatti S, Lojcono A, Faden D. 2006. Autoimmunity and pregnancy: autoantibodies and pregnancy in rheumatic diseases. *Ann N Y Acad Sci*. 1069:346–352.
- Voigt T. 1989. Development of glial cells in the cerebral wall of ferrets: direct tracing of their transformation from radial glia into astrocytes. *J Comp Neurol*. 289(1):74–88.
- Weissman T, Noctor SC, Clinton BK, Honig LS, Kriegstein AR. 2003. Neurogenic radial glial cells in reptile, rodent and human: from mitosis to migration. *Cereb Cortex*. 13(6):550–559.